

## MULTIPARTICLE PRODUCTION IN 340 GeV $\pi^-$ -NUCLEUS COLLISIONS

BY TAUSEEF AHMAD, M. TARIQ, M. IRFAN, M. ZAFAR, M. Z. AHSAN AND M. SHAFI

Department of Physics, Aligarh Muslim University, Aligarh — 202 002, India

(Received November 2, 1988; revised version received January 24, 1989)

A study of the emission characteristics of secondary particles produced in 340 GeV  $\pi^-$ -nucleus interactions has been carried to examine some important features of grey particle production obtained experimentally. The values of emission characteristics are compared with the predictions of various models on the dynamics of strong interactions. Results on the multiplicity of relativistic particles are also presented. The values of the mean normalized multiplicity,  $R_A$ , estimated in terms of the created charged particles reveal a new kind of scaling in hadron-nucleus interactions at high energies.

PACS numbers: 13.85.Hd

### 1. Introduction

During the recent years studies on the disintegrations of nuclei caused by energetic hadrons have become an interesting field of investigation because of the fact that nuclei are regarded as the targets of considerable spatial dimensions and hence may serve as the analyzer of space-time development of the multi-hadronic states produced [1]. Although a number of attempts have been made to investigate some salient features of p-A interactions in the entire range of accelerator energies, yet the investigations on  $\pi^-$ -A interactions are only a few. Furthermore, majority of the experiments on  $\pi^-$ -A collisions have been carried around 200 GeV incident energy [2–4] and only a few attempts [5–8] have been made to study the characteristics of  $\pi^-$ -A collisions at still higher energies. It was, therefore, considered worthwhile to examine in detail some interesting aspects of multiparticle production in 340 GeV  $\pi^-$ -emulsion interactions.

### 2. Experimental details

A stack of Ilford G<sub>5</sub> emulsion, exposed to 340 GeV negative pions at CERN SPS has been used. The dimensions of each pellicle are 15 cm  $\times$  6 cm  $\times$  0.06 cm. The beam flux was estimated to be  $\sim 7 \times 10^4$  particles/cm<sup>2</sup>.

A random sample of 637 events having  $N_b \geq 0$ , where  $N_b$  denotes the number of particles with  $\beta \lesssim 0.7$ , were collected for the present study. All the relevant details regarding the scanning procedure, selection criteria, methods of measurements, etc., may be found in our earlier publications [9, 10].

### 3. Experimental results

Values of the mean multiplicities of grey and black particles obtained by various workers for both p-A and  $\pi^-$ -A collisions at different incident energies are presented in Table I along with the values obtained in the present work. It may be seen in the table that the values of the mean multiplicities of grey and black particles,  $\langle N_g \rangle$  and  $\langle N_b \rangle$  obtained in the present study are comparable with those reported by El-Nadi et al. [7] and Ahmad et al. [8]. The values of  $\langle N_g \rangle$ ,  $\langle N_b \rangle$  and  $\langle N_g \rangle / \langle N_b \rangle$  are observed to be independent of incident energy for both p-A and  $\pi^-$ -A interactions in the energy range  $\sim (17-400)$  GeV [11, 12], whereas El-Nadi et al. [7] and Azimov et al. [13] have reported that  $\langle N_g \rangle$  decreases with increasing energy,  $E_0$ , as:

$$\langle N_g \rangle = 4.06 - 0.26 \ln E_0 \quad (1)$$

for p-A interactions in the energy range  $\sim (50-200)$  GeV and

$$\langle N_g \rangle = 3.50 - 0.21 \ln E_0 \quad (2)$$

for  $\pi^-$ -A interactions in the energy range  $\sim (50-340)$  GeV.

TABLE I

The average values of the different charged secondaries emitted in pion and proton interactions with emulsion nuclei

Type of interaction	Energy (GeV)	$\langle N_g \rangle$	$\langle N_b \rangle$	$\langle N_g \rangle / \langle N_b \rangle$	Reference
p-nucleus	24	$3.16 \pm 0.11$	$4.45 \pm 0.13$	$0.71 \pm 0.03$	[12]
	50	$3.19 \pm 0.12$	$4.34 \pm 0.13$	$0.74 \pm 0.04$	[12]
	200	$2.96 \pm 0.15$	$4.09 \pm 0.18$	$0.72 \pm 0.05$	[12]
	200	$2.70 \pm 0.06$	$5.00 \pm 0.10$	$0.54 \pm 0.02$	[7]
	400	$3.14 \pm 0.14$	$4.22 \pm 0.16$	$0.74 \pm 0.04$	[12]
	400	$3.02 \pm 0.05$	$4.83 \pm 0.07$	$0.63 \pm 0.02$	[18]
	400	$2.99 \pm 0.06$	$5.00 \pm 0.09$	$0.60 \pm 0.02$	[7]
$\pi^-$ -nucleus	50	$2.61 \pm 0.13$	$4.02 \pm 0.15$	$0.65 \pm 0.04$	[12]
	200	$2.86 \pm 0.11$	$4.25 \pm 0.14$	$0.67 \pm 0.03$	[12]
	200	$2.38 \pm 0.04$	$4.52 \pm 0.07$	$0.53 \pm 0.01$	[7]
	300	$2.08 \pm 0.06$	$4.89 \pm 0.11$	$0.43 \pm 0.02$	[5]
	340	$2.25 \pm 0.10$	$5.69 \pm 0.11$	$0.40 \pm 0.02$	[7]
	340	$2.23 \pm 0.06$	$5.80 \pm 0.09$	$0.38 \pm 0.03$	present work
	340	$1.98 \pm 0.06$	$5.30 \pm 0.13$	$0.37 \pm 0.04$	[8]

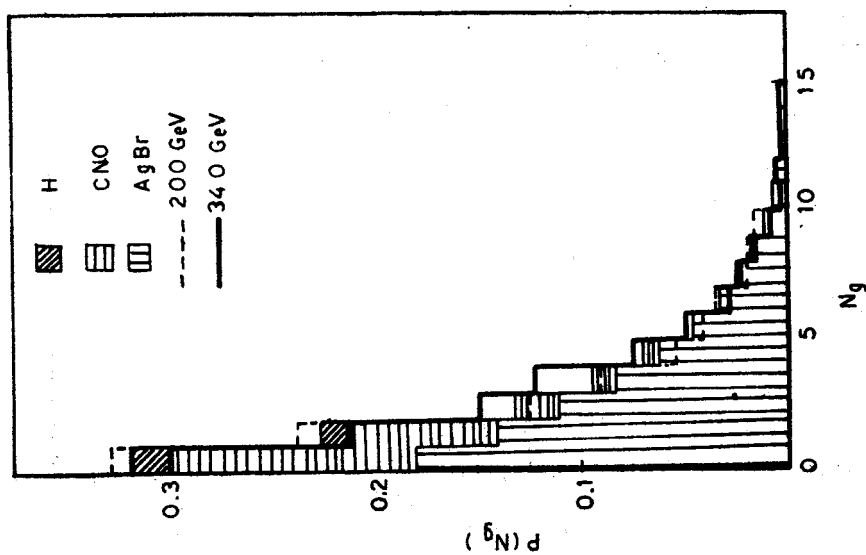


Fig. 1

Fig. 1. Multiplicity distribution of grey tracks in pion nucleus interactions at 200 and 340 GeV. The shaded areas represent the prediction of Stenlund and Otterlund model

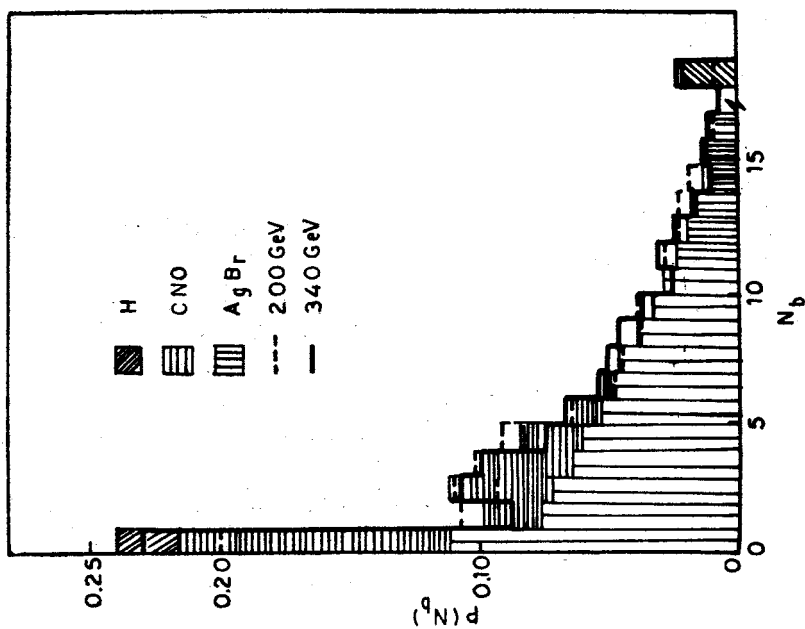


Fig. 2

Fig. 2. Distribution of the number of black tracks at 200 and 340 GeV. The shaded areas correspond to the prediction of the model [15]

It may be noted in Table I that the values of  $\langle N_g \rangle$  for p-A interactions are somewhat higher than the corresponding values obtained for  $\pi^-$ -A collisions at the same incident energy. The values of the ratio  $\langle N_g \rangle_{\pi^-A} / \langle N_g \rangle_{pA}$  have been reported [7, 12] to be  $0.82 \pm 0.05$  and  $0.88 \pm 0.02$  at 50 and 200 GeV respectively. These values are, thus, quite close to the value of the ratio of the mean numbers of encounters  $\langle \nu \rangle_{\pi^-A} / \langle \nu \rangle_{pA} = 0.85$ , where  $\langle \nu \rangle = A \sigma_{h-p}^{inel} / \sigma_{h-A}^{inel}$ ,  $\sigma_{h-p}^{inel}$  and  $\sigma_{h-A}^{inel}$  denote the inelastic cross-sections for hadron-proton and hadron-nucleus collisions, respectively. The values of  $\sigma_{h-p}^{inel}$  have been reported [14] to be  $(32.3 \pm 0.8)$  and  $(21.2 \pm 0.3)$  mb for proton and  $\pi^-$ -projectiles respectively, whereas the values of  $\sigma_{h-A}^{inel}$  are found to be  $46A^{0.69}$  and  $28A^{0.75}$  for p-A and  $\pi^-$ -A interactions, respectively, where  $A$  is the target mass.

Recently, Stenlund and Otterlund [15] have proposed a model to explain the production of slow particles (particles with  $\beta \lesssim 0.7$ ). This model explains the behaviour of the multiplicity distributions of black, grey and heavily ionizing particles and their inter-correlations. The model also predicts that any of the three multiplicities —  $N_b$ ,  $N_g$  and  $N_h$  — may be used to estimate the mean number of intranuclear collisions with almost equal reliability.

Multiplicity distributions of black, grey and heavily ionizing particles obtained in 340 GeV  $\pi^-$ -A interactions are compared with the predictions of the Stenlund and Otter-

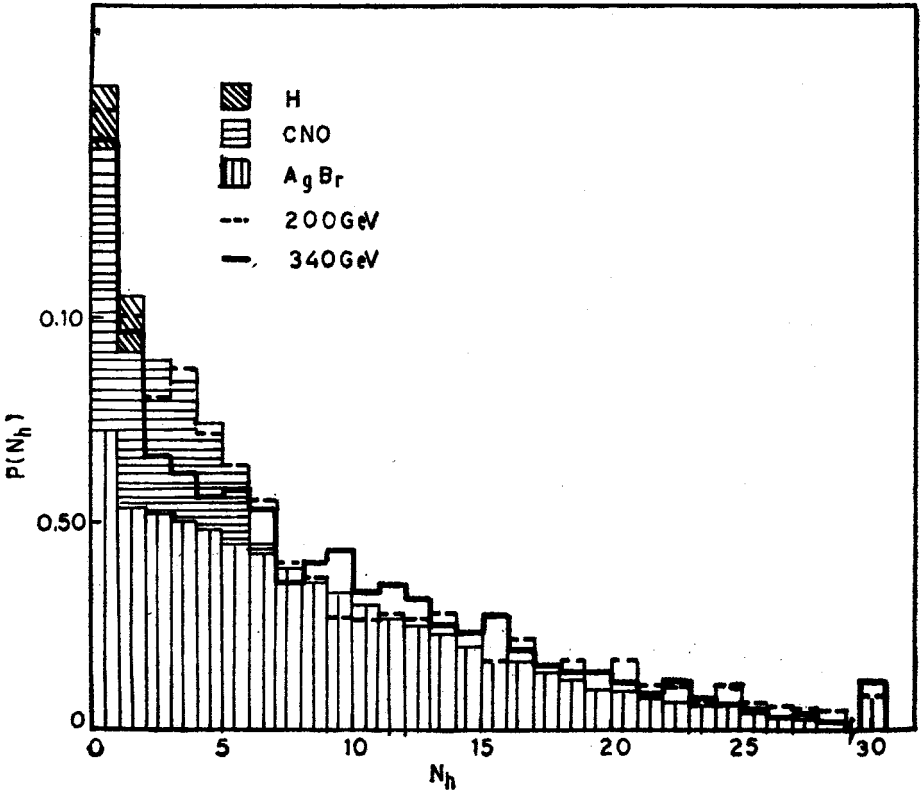


Fig. 3.  $N_h$ -distribution at 200 and 340 GeV. The shaded areas correspond to the prediction of the model [15]

lund model [15] in Figs. 1–3. The agreement between the experimental distribution and the distribution obtained theoretically is quite good. In Figs. 4 and 5, the variations of  $\langle N_g \rangle$  with  $N_b$  and  $\langle N_b \rangle$  with  $N_g$  are plotted for 340 GeV  $\pi$ -A interactions respectively. It may be seen in the figures that  $\langle N_g \rangle$ - $N_b$  correlation is observed to saturate beyond  $N_b \sim 9$ , whereas the correlation  $\langle N_b \rangle$ - $N_g$  agrees with the prediction of the model [15]. It has also been pointed out by Stenlund and Otterlund [15] that saturation in  $\langle N_g \rangle$ - $N_b$  correlation should occur because the energy of the struck nucleus becomes so large that there is no way to dispose it off except by undergoing total destruction. When such a situation arise, then it is expected that: (i) the emitted products may have higher energies than the particles envisaged to be produced through the evaporation process, which in turn leads to an increase in the grey particle multiplicity and (ii) relatively heavier fragments might be produced during the evaporation process causing a decrease in the multiplicity of the black tracks.

Variation of the mean multiplicity of charged shower particles,  $\langle N_s \rangle$ , their dispersion,  $D(N_s)$  and the ratio,  $D(N_s)/\langle N_s \rangle$  with  $\langle v(N_g) \rangle$  and  $\langle v(N_b) \rangle$  are plotted in Fig. 6:  $\langle v(N_g) \rangle$  and  $\langle v(N_b) \rangle$  represent respectively the mean numbers of the intranuclear collisions estimated by using the grey and black particle multiplicities. The values of  $\langle v(N_g) \rangle$  and  $\langle v(N_b) \rangle$  are obtained with the help of the following relation:

$$\langle v(N_x) \rangle = C_0 + C_1 N_x^{1/2} + C_2 N_x + C_3 (N_x)^{3/2} \quad (3)$$

where  $N_x$  denotes  $N_g$ ,  $N_b$  or  $N_h$ . The values of the coefficients,  $C_0$ ,  $C_1$ ,  $C_2$  and  $C_3$  acquire different values for  $N_g$ ,  $N_b$  and  $N_h$ . The values of these coefficients have been obtained by Stenlund and Otterlund [15] for both p-A and  $\pi$ -A interactions.

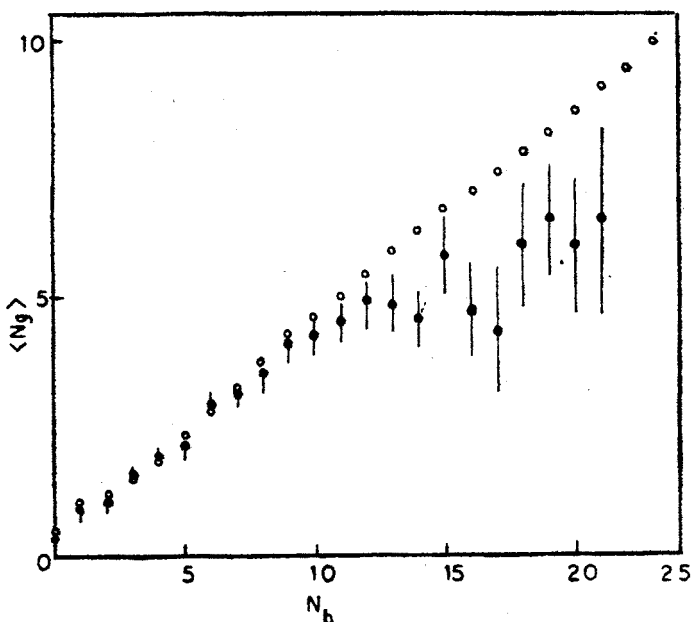


Fig. 4. Variation of  $\langle N_g \rangle$  with  $N_b$  at 340 GeV. The solid circles are the experimental points and the open circles are the prediction of the model [15]

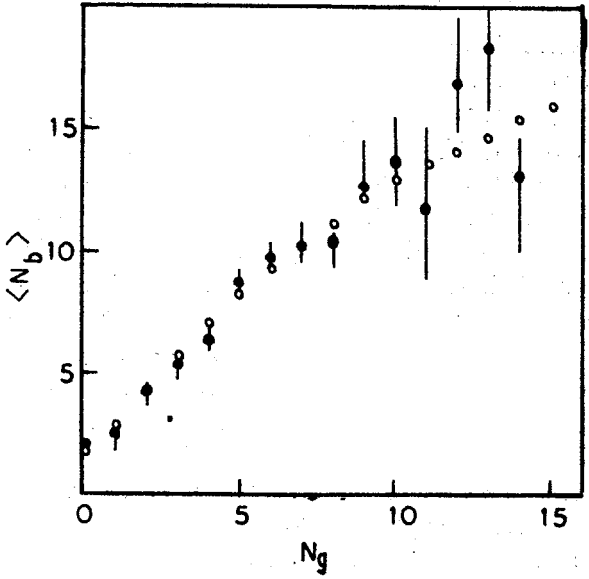


Fig. 5. Variation of  $\langle N_b \rangle$  with  $N_g$  at 340 GeV. The points are discussed in Fig. 4

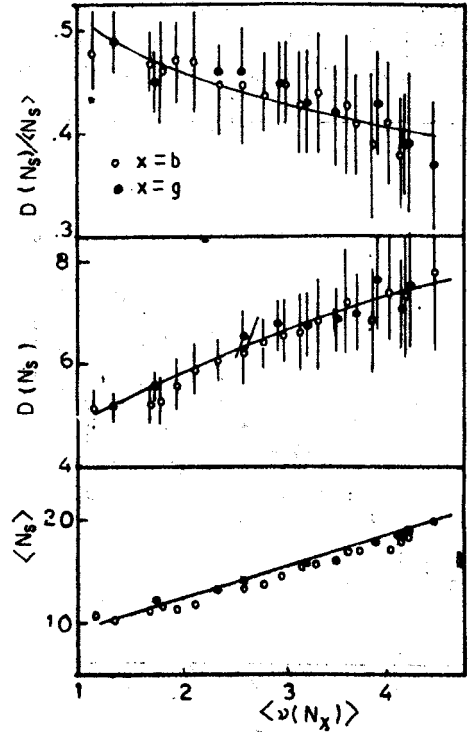


Fig. 6. Variation of  $\langle N_s \rangle$ ,  $D(N_s)$  and the ratio  $D(N_s)/\langle N_s \rangle$  with  $\langle \nu(N_g) \rangle$  and  $\langle \nu(N_b) \rangle$  for  $\pi$ -nucleus interactions at 340 GeV. The open points correspond to the black tracks and the solid points to the grey tracks

It is interesting to note in Fig. 6 that the data points for  $\langle v(N_g) \rangle$  and  $\langle v(N_b) \rangle$  fall on a single curve in each case. This observation, therefore, reveals that  $N_g$  and  $N_b$  may be used as a good measure of the mean number of hadron-nucleon collisions inside the nucleus with almost equal reliability. It has been suggested [16] that  $\langle N_s \rangle$  and  $D(N_s)$  vary with the mean number of intranuclear collisions,  $\langle v \rangle$ , as:

$$\langle N_s \rangle = a\langle v \rangle + b, \quad (4)$$

$$D^2(N_s) = c\langle v \rangle + d. \quad (5)$$

The best fits to the experimental data on 340 GeV  $\pi^-$ -A interactions are obtained to be of the following forms

$$\langle N_s \rangle = (2.77 \pm 0.14) \langle v(N_g) \rangle + (7.03 \pm 0.47) \quad (6)$$

$$D^2(N_s) = (10.23 \pm 0.89) \langle v(N_g) \rangle + (13.84 \pm 2.94) \quad (7)$$

A KNO scaling [17] type fit has been tried to explain the multiplicity distribution of grey particles produced in  $\pi^-$ -A and p-A interactions by plotting the variation of  $P(N_g) \times 2\langle N_g \rangle$  with  $N_g/\langle N_g \rangle$  in Fig. 7. It is interesting to see in the figure that the data points obtained for both p-A and  $\pi^-$ -A collisions at different energies are nicely reproduced by

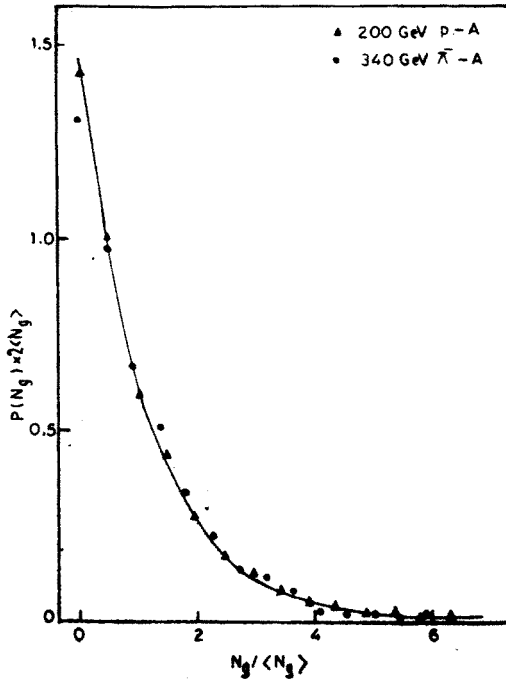


Fig. 7. Variation of  $P(N_g) \times 2\langle N_g \rangle$  with  $N_g/\langle N_g \rangle$  at 200 GeV p-A and 340 GeV  $\pi^-$ -A. The curve is explained in the text

the curve obtained by using the following relation

$$P(N_g) \times 2 \langle N_g \rangle = e^{-N_g / \langle N_g \rangle}. \tag{8}$$

It should be noted that relation (8) is quite close to the theoretically predicted distribution [7] given by

$$P(N_g) \times 2 \langle N_g \rangle = e^{-N_g / 2 \langle N_g \rangle}. \tag{9}$$

The angular distributions of grey particles obtained for CNO, AgBr and emulsion groups of interactions at 340 GeV are plotted in Fig. 8. The curve in Fig. 8b corresponds to the predictions of the additive quark model [12] (AQM). It may be seen in the figure that the angular distribution of grey particles depends weakly on the mass of the target nucleus in such a way that comparatively more grey particles appear in the forward hemisphere ( $\theta < \pi/2$ ) for the lighter targets. The values of the coefficients of angular asymmetry,  $k$ , defined as

$$k = N_1 / N_2, \tag{10}$$

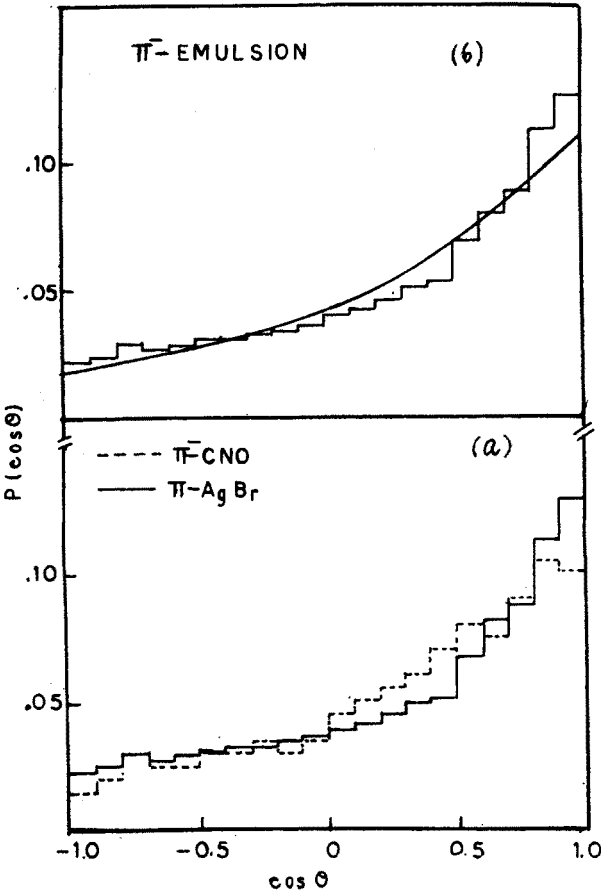


Fig. 8. Angular distribution of grey particles at 340 GeV for (a)  $\pi^-$ -CNO and  $\pi^-$ -AgBr collisions and (b)  $\pi^-$ -emulsion nuclei. The curve in (b) shows the AQM prediction



where  $N_1$  and  $N_2$  are the total number of grey particles emitted in the forward and backward hemispheres, respectively, are found to be  $3.09 \pm 0.12$ ,  $2.36 \pm 0.06$  and  $2.27 \pm 0.08$  for  $\pi^-$ -CNO,  $\pi^-$ -emulsion and  $\pi^-$ -AgBr collisions. The values of  $k$  for p-CNO, p-emulsion and p-AgBr collisions have been reported [18] to be  $3.13 \pm 0.10$ ,  $2.34 \pm 0.07$  and  $2.23 \pm 0.09$  respectively. This trend of decrease in the value of  $k$  with increasing target size also reveals that the angular distribution of grey particles depends on the mass of the struck nucleus. The value of  $k$  has, however, been reported to remain independent of the energy and identity of the colliding hadron [12]. Furthermore, the values of  $k$  are found to be 2.36 and 2.34 for 340 GeV  $\pi^-$ -A and 400 GeV p-A collisions respectively which are in excellent agreement with the value  $\sim 2.4$ , predicted by the AQM [12].

Dependence of  $\langle \cos \theta \rangle$  and  $D(\cos \theta)$ , where  $\theta$  is the emission angle of a grey track with respect to the mean direction of the projectile in the lab frame, on the multiplicity of grey and black particles,  $N_g$  and  $N_b$ , are plotted in Fig. 9. It may be seen in the figure that  $\langle \cos \theta \rangle$  decreases while  $D(\cos \theta)$  increases with  $N_g$  and  $N_b$  upto  $\sim N_g$  ( $N_b$ )  $\leq 8$  and thereafter the two parameters acquire almost constant values. It is interesting to note that at the same value of  $N_b$ , saturation in  $\langle N_g \rangle$ - $N_b$  correlation has been observed in the present study. Similar dependence of  $\langle \cos \theta \rangle$  and  $D(\cos \theta)$  on  $N_g$  and  $N_b$  were also observed earlier [12, 18] in the case of p-A interactions.

An important parameter which provides a means of distinguishing between various theoretical models is the mean normalized multiplicity,  $R_A$ , defined as

$$R_A = \langle N_s \rangle / \langle N_{ch} \rangle, \quad (11)$$

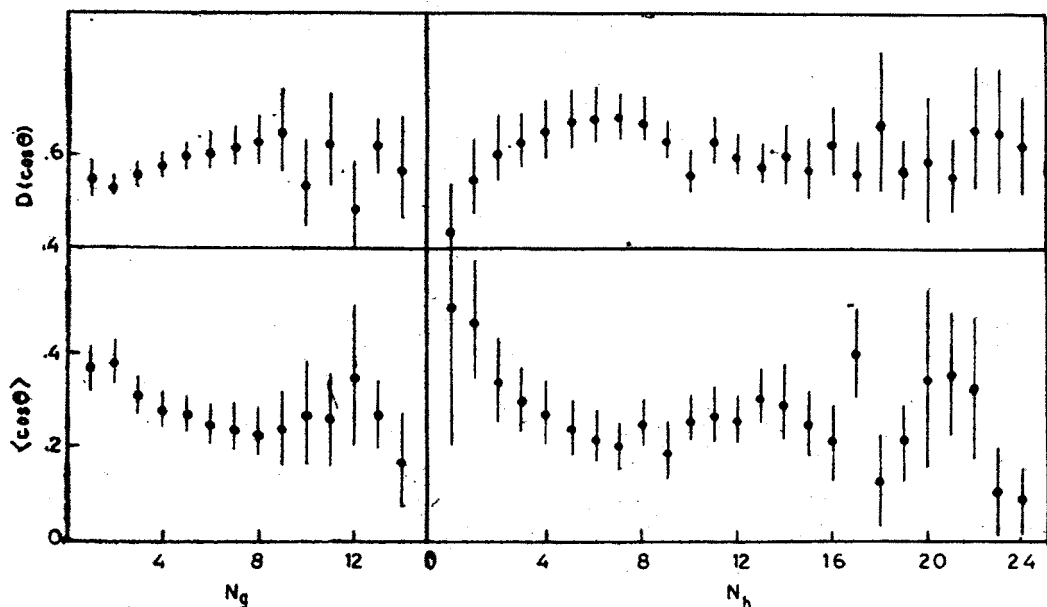


Fig. 9. Variation of  $\langle \cos \theta \rangle$  and  $D(\cos \theta)$  with the multiplicity of grey and black tracks

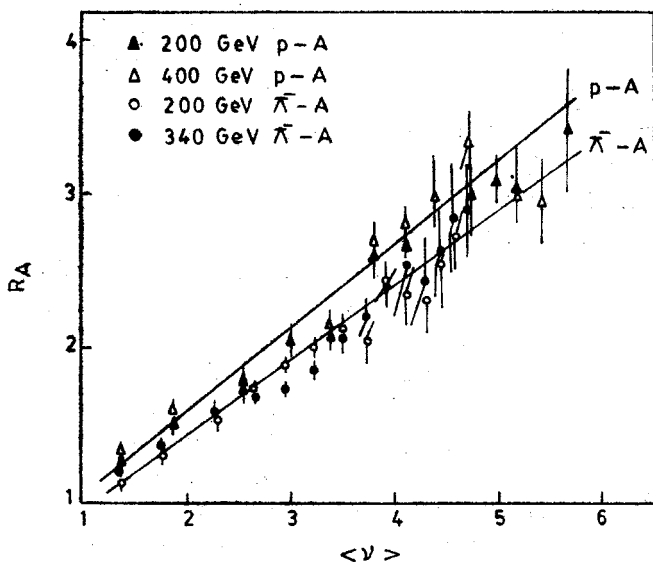


Fig. 10. Variation of  $R_A$  with  $\langle \nu \rangle$ . The lines are the best fit to the data

where  $\langle N_s \rangle$  and  $\langle N_{ch} \rangle$  are the mean multiplicities of relativistic particles produced in hadron-nucleus and hadron-proton collisions at the same incident energy. For examining the dependence of  $R_A$  on the mean number of intranuclear collisions, variation of  $R_A$  with  $\langle \nu \rangle$  is plotted for 200 and 340 GeV  $\pi^-$ -nucleus and 200 and 400 GeV p-nucleus interactions in Fig. 10. The best fits to the experimental data are found to be

$$R_A = (0.540 \pm 0.037) \langle \nu \rangle + (0.490 \pm 0.153) \quad (12)$$

for p-A collisions and

$$R_A = (0.472 \pm 0.021) \langle \nu \rangle + (0.469 \pm 0.074) \quad (13)$$

for  $\pi^-$ -A collisions.

From the above equations it is clear that  $R_A$ - $\langle \nu \rangle$  relationships are different for p-A and  $\pi^-$ -A interactions.

It has been suggested by several workers [9, 14, 19] that better agreement between the experimental and predicted behaviour of the mean normalized multiplicity may be obtained if this parameter is re-defined by considering only the created charged particles as [14]

$$R_4 = (\langle N_s \rangle - \alpha_A) / (\langle N_{ch} \rangle - \alpha_H), \quad (14)$$

where  $\alpha_A$  and  $\alpha_H$  are the leading particle multiplicities in hadron-nucleus and hadron-proton collisions. The values of  $\alpha_A$  have been reported [19] to be 0.67 and 0.50 for p-A and  $\pi^-$ -A interactions whereas the values of  $\alpha_H$  for p-p and  $\pi^-$ -p collisions have been found [14] to be 0.9 and 1.4 respectively.

Variation of  $R_4$  with  $\langle \nu \rangle$  is shown in Fig. 11 for both p-A and  $\pi^-$ -A interactions at 200 and 340 GeV respectively. It may be seen in the figure that the experimental points

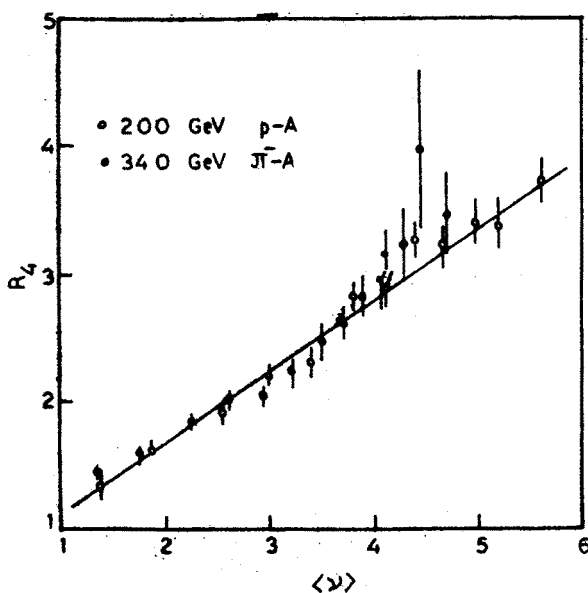


Fig. 11. Dependence of  $R_4$  with  $\langle \nu \rangle$

obtained for both types of interactions lie on a single straight line. The least squares fit, to the data is found to be

$$R_4 = (0.57 \pm 0.04) \langle \nu \rangle + (0.52 \pm 0.04). \quad (15)$$

These observations, therefore, suggest that  $R_4$  increases with the mean number of intra-nuclear collisions in almost similar fashion irrespective of the energy and nature of the incident hadron, thus indicating a new kind of scaling in hadron-nucleus interactions.

### 5. Conclusions

Based on the findings of the present study, following conclusions may be drawn:

1. Multiplicity distributions of grey, black and heavily ionizing particles and the behaviour of the inter-correlations amongst these parameters are in fine agreement with the predictions of the Stenlund and Otterlund model. It is also observed that both  $N_g$  and  $N_b$  may be regarded as a reasonable measures of the mean number of hadron-nucleon collisions inside the struck nucleus.

2. The behaviour of the correlations between grey and black particle multiplicities, i.e.  $\langle N_b \rangle - N_g$  correlation is found to be nicely described by the predictions of the Stenlund and Otterlund model. It is also observed that any of the three multiplicities,  $N_g$ ,  $N_b$  or  $N_h$ , may be used to estimate the mean number of intranuclear collisions with almost equal reliability.

3. The angular characteristics of grey particles are nicely explained by using the predictions of the Additive Quark Model.

4. Almost similar nature of the dependence of the mean normalized multiplicity, estimated by considering only the created charged particles on  $\langle v \rangle$  observed for both p-A and  $\pi$ -A collisions indicate a new kind of scaling in hadron-nucleus collisions.

#### REFERENCES

- [1] W. Busza, *Acta Phys. Pol.* **B8**, 333 (1977); V. R. Zoller, N. N. Nikolayev, *Sov. J. Nucl. Phys.* **38**, 538 (1982).
- [2] Z. V. Anzon et al., *Nucl. Phys.* **B129**, 205 (1977).
- [3] J. E. Elias et al., *Phys. Rev.* **D22**, 13 (1980).
- [4] M. A. Faessler et al., *Nucl. Phys.* **B157**, 1 (1979).
- [5] J. Babecki et al., *Acta Phys. Pol.* **B16**, 322 (1985).
- [6] R. Holyński et al., *Acta Phys. Pol.* **B17**, 201 (1986).
- [7] M. El-Nadi et al., *Phys. Rev.* **D27**, 12 (1983).
- [8] Shafiq Ahmad et al., *Nucl. Phys.* **B254**, 441 (1985).
- [9] A. Shakeel et al., *Nuovo Cimento* **76A**, 699 (1982).
- [10] M. Irfan et al., *Phys. Rev.* **D30**, 218 (1984).
- [11] J. Babecki, G. Nowak, *Acta Phys. Pol.* **B9**, 401 (1978).
- [12] S. A. Azimov et al., *Nuovo Cimento* **84A**, 117 (1984).
- [13] S. A. Azimov et al., *J. Phys. G* **4**, 813 (1978).
- [14] H. Khushnood et al., *Can. J. Phys.* **61**, 1120 (1983).
- [15] E. Stenlund, I. Otterlund, *Nucl. Phys.* **B198**, 407 (1982).
- [16] C. De Marzo et al., *Phys. Rev.* **D29**, 2476 (1984).
- [17] Z. Koba et al., *Nucl. Phys.* **B40**, 317 (1972).
- [18] A. Shakeel, Ph. D. Thesis, A.M.U., Aligarh, India.
- [19] T. Aziz et al., *Indian J. Pure Appl. Phys.* **18**, 778 (1980).